Simulation of the thermodynamics and removal processes in the sulfate-ammonia-nitric acid system during winter: Implications for $PM_{2.5}$ control strategies

Dimitris V. Vayenas,[1] Satoshi Takahama,[2] Cliff I. Davidson,[3,4] and Spyros N. Pandis[2,4]

Received 19 May 2004; revised 19 November 2004; accepted 28 December 2004; published 18 March 2005.

[1] In the eastern United States, inorganic species account for approximately half of the $PM_{2.5}$ mass, with sulfate salts comprising the largest fraction. Current strategies for reducing $PM_{2.5}$ mass concentrations target reducing SO_2 to reduce sulfate, but in such a case more ammonium nitrate may form when nitric acid is present. Large-scale chemical transport models suffer from uncertainties associated with emission inventories. To examine how the inorganic $PM_{2.5}$ concentration responds to changes in emissions, we introduce an observation-based box model, the thermodynamic model with removal (TMR), to estimate responses of $PM_{2.5}$ to precursor concentrations. TMR assumes that particles are in equilibrium with the gas phase, but the removal rate of total ($PM_{2.5}$ + gas) nitric acid from the system depends on the gas/aerosol partitioning of this species. The model is used to investigate sulfate, total ammonia, and total nitric acid control strategies for western Pennsylvania during the winter using measurements obtained in the Pittsburgh Air Quality Study. Predictions from TMR are compared with observations and predictions of a chemical equilibrium model (GFEMN), where the perturbation of sulfate or total ammonia does not affect the total nitric acid availability. Results show that TMR predicts more aerosol nitrate to form than GFEMN in scenarios where the total ammonia to sulfate ratio is increased, but model results are similar under ammonia-limited conditions. When sulfate is reduced by 50% during the winter, GFEMN predicts that inorganic $PM_{2.5}$ mass concentrations will be reduced by 23%, while TMR predicts that there will only be an 8% reduction. For a 50% reduction in ammonia availability, inorganic $PM_{2.5}$ was reduced by 29%, while for a 50% reduction in total nitric acid a 17% reduction in inorganic $PM_{2.5}$ was predicted. The analysis suggests the importance of the phase state of the aerosol for the effectiveness of the emission control strategies.

Citation: Vayenas, D. V., S. Takahama, C. I. Davidson, and S. N. Pandis (2005), Simulation of the thermodynamics and removal processes in the sulfate-ammonia-nitric acid system during winter: Implications for $PM_{2.5}$ control strategies, *J. Geophys. Res.*, *110*, D07S14, doi:10.1029/2004JD005038.

1. Introduction

[2] Atmospheric particles have adverse effects on human health and directly affect visibility, air quality and climate change [*North American Research Strategy for Tropospheric Ozone* (*NARSTO*), 2003; *Intergovernmental Panel on Climate Change* (*IPCC*), 2001]. The U.S. EPA has promulgated regulations regarding mass concentrations of fine particulate matter (PM), which are particles with aerodynamic diameters less than 2.5 μm ($PM_{2.5}$), to alleviate the health and economic burdens attributed to high concentrations of particulate matter. $PM_{2.5}$ consists of many different types of particles covering a broad range of composition and size and can be categorized into primary and secondary. Primary aerosols include automobile exhaust, industrial emissions but also sea spray and dust, and are emitted directly into the atmosphere. Secondary aerosols, which generally have diameters less than 2.5 μm, are produced in the atmosphere from reactions involving primary and secondary gases [*Pandis and Seinfeld*, 1998].

[3] In the eastern United States, inorganic species account for approximately half of the $PM_{2.5}$ mass, with sulfate salts constituting the largest fraction [*U.S. Environmental Protection Agency*, 1996]. The sources of these particles and precursor gases are known to be primarily anthropogenic, and are obvious targets for emission controls. Oxidation of SO_2 is the primary source of sulfate, and current control strategies for reducing $PM_{2.5}$ target this emission source. Ammonium and nitrate are also significant contributors to inorganic $PM_{2.5}$ mass, and their sources are primarily

[1]Department of Environmental and Natural Resources Management, University of Ioannina, Agrinio, Greece.
[2]Department of Chemical Engineering, Carnegie Mellon University, Pittsburgh, Pennsylvania, USA.
[3]Department of Civil and Environmental Engineering, Carnegie Mellon University, Pittsburgh, Pennsylvania, USA.
[4]Also at Department of Engineering and Public Policy, Carnegie Mellon University, Pittsburgh, Pennsylvania, USA.

0148-0227/05/2004JD005038$09.00

agricultural sources and NO_x from traffic and power generation emissions, respectively. Because of the interactions among these species, reduction of sulfate may result in the increase of nitrate [*Ansari and Pandis*, 1998].

[4] Our objective is to understand how the inorganic $PM_{2.5}$ mass responds to changes in emissions and provide a means by which alternative emission control strategies can be evaluated. Conceptually, three-dimensional chemical transport models are well suited for this purpose as they link emissions to $PM_{2.5}$ concentrations directly through detailed descriptions of the physics and chemistry of the atmosphere. However, at this time such models suffer from large uncertainties associated with emission inventories of primary $PM_{2.5}$ and precursor gases [*Seigneur*, 2001]. As such, alternative approaches have been proposed, including observation-based approaches or methods combining measurements with models [e.g., *Russell and Cass*, 1986; *Ansari and Pandis*, 1998; *Pun and Seigneur*, 2001].

[5] In particular, aerosol models relying on thermodynamic equilibrium principles to predict the composition and physical state of inorganic atmospheric aerosols have been in development for the past 20 years [*Bassett and Seinfeld*, 1983; *Saxena et al.*, 1986; *Pilinis and Seinfeld*, 1987; *Kim et al.*, 1993; *Meng et al.*, 1995; *Jacobson et al.*, 1996; *Nenes et al.*, 1999; *Ansari and Pandis*, 1999; *Wexler and Clegg*, 2002]. These have been incorporated as modules in large-scale models to predict the partitioning of condensable compounds between the gas and particle phases, but researchers have also used these thermodynamic models alone to conduct investigations of inorganic $PM_{2.5}$ response to changes in precursor concentrations [*Ansari and Pandis*, 1998; *West et al.*, 1999; *Blanchard and Hidy*, 2003]. Precursor species of inorganic $PM_{2.5}$ include sulfuric acid, ammonia and nitric acid, and are used by the model to calculate the aerosol fraction of these species. Sulfuric acid exists almost entirely in the aerosol phase in a neutralized form, but ammonia and nitric acid can be found in both aerosol and gas phases. Ammonia is the predominant basic gas in the atmosphere and neutralizes sulfuric acid and nitric acid to form aerosols, and small quantities can also be absorbed into liquid aerosols by quantities governed by considerations of vapor-liquid equilibrium. Nitric acid generated in the gas phase can lead to aerosol nitrate formation by two pathways: nitric acid can be neutralized by ammonia to form liquid or solid aerosols, and it can also be incorporated into liquid aerosols by amounts determined by the composition of the particle.

[6] Evaluating emission control strategies with these thermodynamic models, however, makes the implicit assumption that while the concentration of one species is varied, the availability of other precursors remains constant, which may not always be the case. *Pandis and Seinfeld* [1990] showed that the partitioning of semivolatile species between the gas and aerosol phases can affect their lifetime in the atmosphere. For instance, nitric acid vapor has a much shorter residence time in the atmosphere than aerosol nitrate, and a reduction in sulfate may increase the amount of free ammonia and hence the amount of nitrate partitioned into the aerosol phase. In such a case the concentration of total nitric acid will not remain constant but instead increase, thereby increasing the potential to contribute to the formation of $PM_{2.5}$.

[7] The present work introduces an Eulerian box model that relies only on observation-based inputs of $PM_{2.5}$ precursor concentrations and accounts for the variable deposition rates between aerosol nitrate and gas-phase nitric acid. The predictions by this model are evaluated for a winter month in the western Pennsylvania region, where meteorological conditions and atmospheric compositions favored aerosol nitrate formation. The predicted responses of the $PM_{2.5}$ to emission changes are presented alongside predictions made with the traditional thermodynamic approach of *Ansari and Pandis* [1998] alone, and the significance of integrating removal processes with an equilibrium module is illustrated.

2. Measurements From the Pittsburgh Air Quality Study (PAQS)

[8] Measurements of gases, aerosols, and meteorological conditions were taken between July 2001 to August 2002 for the Pittsburgh Air Quality Study (PAQS). The monitoring site was located atop a hill in Schenley Park, an urban area approximately 6 km from downtown Pittsburgh, PA, and several hundred meters from any major sources. The city is located in the northeastern United States, in between utility and agricultural emission sources in the Midwest and large urban centers found along the east coast. The average $PM_{2.5}$ mass concentration as measured by the Federal Reference Method was 12 $\mu g/m^3$ during the winter with sulfate and nitrate constituting 25% and 17% of the mass during this period [*Rees et al.*, 2004]. Concentrations of crustal elements in $PM_{2.5}$ were generally less than 0.2 $\mu g/m^3$ and constituted a small fraction of aerosol mass. Crustal elements in the coarse fraction were also less than 0.2 $\mu g/m^3$ on average. Data for temperature (T), relative humidity (RH), total ($PM_{2.5}$ + gas) ammonia (TA), total ($PM_{2.5}$ + gas) nitric acid (TN), and $PM_{2.5}$ sulfate (TS) were collected and corrected by the methods described by *Wittig et al.* [2004a, 2004b] and *Takahama et al.* [2004].

[9] For this study, hourly measurements made during January 2002 were aggregated to obtain average hourly values of T, RH, TA, TN, TS, and aerosol nitrate to construct a diurnal profile of these components for an "average day" in January (Figure 1). Error bars, representing the spread of the measurements one standard deviation from the monthly mean in both directions, show that there is a lot of variability over the entire month, but the diurnal trend represented by the mean is preserved. Mean values of the six parameters listed above for the aggregated period in January are as follows: T = 3.0°C, RH = 68%, TA = 1.7 $\mu g/m^3$, TN = 3.0 $\mu g/m^3$, TS = 3.0 $\mu g/m^3$, and $PM_{2.5}$ nitrate = 2.1 $\mu g/m^3$. The average molar ratio of aerosol ammonium to sulfate for the month was 2.9, indicating that generally, sulfate was fully neutralized and existed as ammonium sulfate. The temperature exhibited a daytime peak and low values in the evening and early morning, and the relative humidity followed an inverted pattern of the temperature. Sulfate in the Pittsburgh region shows on average relatively little variation throughout the day, which is indicative of material transported from outside of the region [*Tang et al.*, 2004]. The total ammonia also shows little variation throughout the day, also indicative of long-range transport, though there is

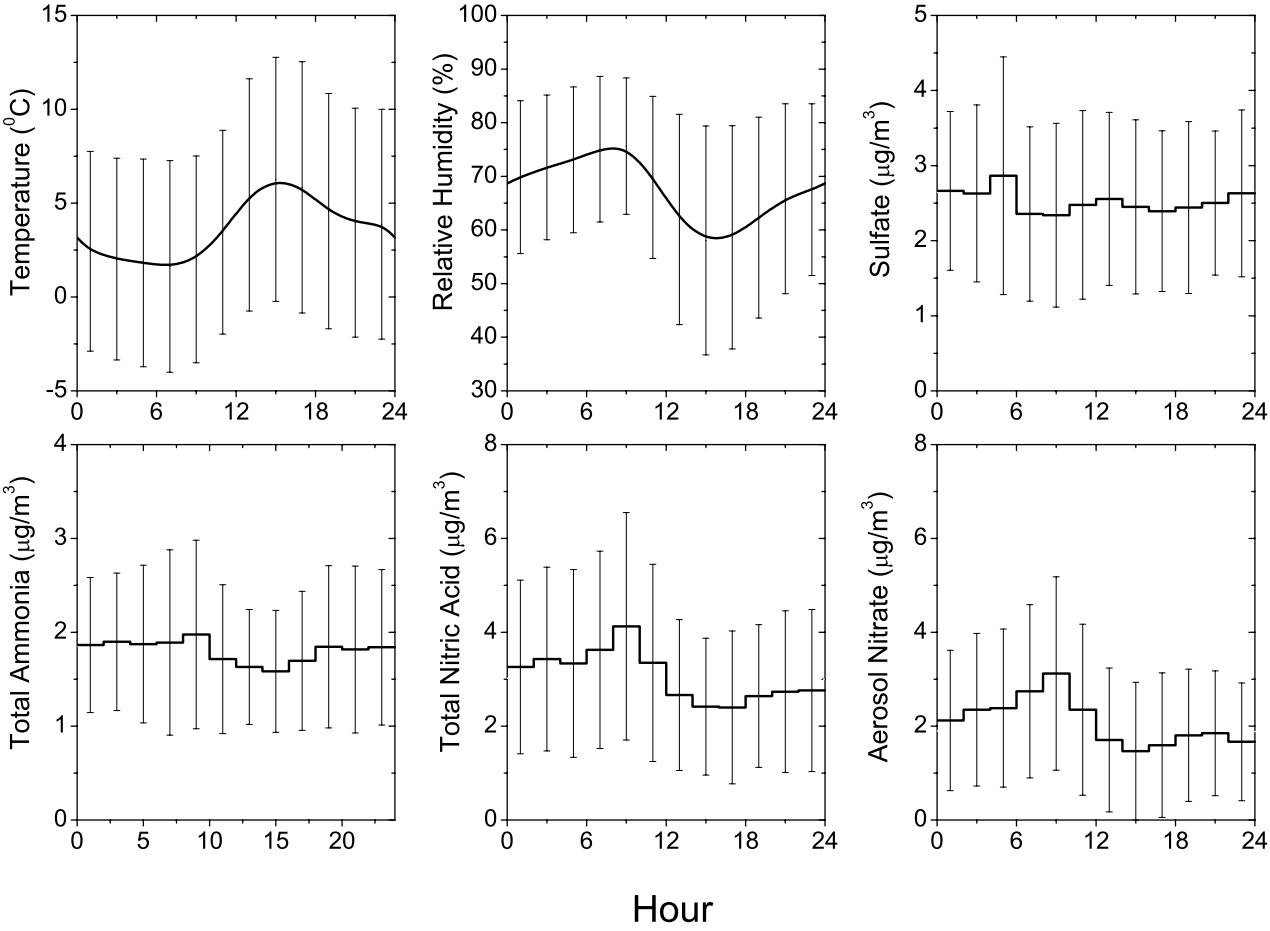

Figure 1. Averages of measured concentrations from the Pittsburgh Air Quality Study during January 2002. Error bars represent ± one standard deviation of the data.

a slight trend of higher concentrations in the evening and lower concentrations during the day. This small variation can be attributed to vertical mixing by changes in the planetary boundary layer height between morning/evening and daylight hours. Total nitric acid also shows a similar diurnal trend, which can be attributed to chemical production and the change in mixing heights in the morning hours. Nitric acid can be produced during the night by reactions of N_2O_5 and water, while limited quantities of ammonia are emitted from local sources. These mechanisms increase the concentrations of these two semivolatile species during the night and early morning while the boundary layer height is low, and the breaking up of the boundary layer after sunrise causes the drop in concentrations during the day. The fraction of nitrate that is in the aerosol phase depends on meteorological conditions, ammonia and nitric acid availability, and also the presence of other compounds in the particle phase. Because of the cold temperatures prevalent in January, a large fraction of the total nitric acid resides in the aerosol phase.

[10] On the basis of aerosol water measurements, *Khlystov et al.* [2005] concluded that in January 2002 particles were generally liquid above and solid below a threshold relative humidity. The threshold was in the 50–60% range [*Takahama et al.*, 2004]. A value of 50% is used as the threshold in this study based on the measurements of *Khlystov et al.* [2005]. The mutual deliquescence RH of ammonium nitrate and ammonium sulfate is generally above 70% for temperatures experienced in January. This suggests that efflorescence and crystallization govern the physical state of the particles. The average RH in January drops to 59% (Figure 1), and as the average RH remains above the critical threshold for crystallization, in the base case all modeled particles are assumed to be liquid. The sensitivity of the model results to this assumption will be explored in a subsequent section.

3. Simulations

[11] For simplicity, only the sulfate/nitrate/ammonium system is considered in this study. For a region with low concentrations of crustal elements, as is the case in the area of our application, this simplification is reasonable. The potential effect of the crustal species on the phase of the ambient aerosol (solid or liquid) is included by the use of the measured phase state [*Khlystov et al.*, 2005]. Two models are used to assess the system response to changes in current emissions: (1) a thermodynamic model (GFEMN) that partitions total ($PM_{2.5}$ + gas) concentrations into gas and aerosol phases using the sulfate, total ammonia, and

total nitric acid concentrations, and (2) a new box model (thermodynamic model with removal (TMR)) that simulates partitioning, emission, chemical production and deposition of total nitric acid while sulfate and total ammonia are obtained from ambient measurements. The main difference between these two models is that the phase partitioning of nitric acid affects the lifetime and therefore the availability of total nitric acid in TMR, while in GFEMN the phase change has no such effect.

[12] Emission changes in SO_2 and ammonia are reflected by changes in the respective concentrations of sulfate and total ammonia. The average mass concentration of $PM_{2.5}$ or a particular component over a 24-hour cycle was used to characterize its response to changes in emissions.

[13] Both models, as applied here, use the following assumptions. Since the input of semivolatile components used by the model is the sum of $PM_{2.5}$ and gas-phase concentrations, the fraction partitioned into coarse mode aerosol is not a consideration for the base case. When the emission changes are simulated, however, we implicitly assume that the fraction partitioned into coarse mode $PM_{2.5}$ remains small. The error introduced by this assumption is expected to be small for areas with low concentrations of coarse-mode crustal elements that would compete for semivolatile species such as nitric acid. Furthermore, the phase state of the particles is assumed to remain constant as the composition of the aerosol is varied. The possibility of a change in phase after changes in emissions will be addressed in the discussion section. In addition, since these two models employ a bulk equilibrium approach, the traditional assumptions when using this method apply: (1) particles are in equilibrium with the gas phase, and (2) the particles are homogeneous and internally mixed. Also, the influence of organics on inorganic thermodynamics is neglected.

3.1. GFEMN Model Formulation

[14] GFEMN [*Ansari and Pandis*, 1999] is a thermodynamic model that partitions total concentrations between gas and aerosol phases to satisfy chemical equilibrium, which corresponds to the minimum Gibbs free energy of the system subject to mass and charge balance constraints:

$$\min\ G = \sum_i \mu_i n_i$$

$$\text{s.t.}\quad \sum_a \nu_a n_a - \sum_c \nu_c n_c = 0$$

$$\mathbf{Wn} = \mathbf{T},$$

where μ is the chemical potential, n the number of moles, and ν the ion charge. The subscript i indicates any chemical species, a indicates anions, and c indicates cations. **W** is a matrix vector of stoichiometric coefficients, **n** the vector of n_i's, and **T** the vector of total concentrations {TA, TN, TS}.

[15] *Takahama et al.* [2004] evaluated this model for the case of western Pennsylvania using semicontinuous measurements from PAQS and determined that $PM_{2.5}$ nitrate prediction errors were on average around 0.5 $\mu g/m^3$, with errors usually lying within the bounds of measurement uncertainties. The measured T, RH, TA, TN, and TS for each hour of the 24-hour cycle are inputs to GFEMN.

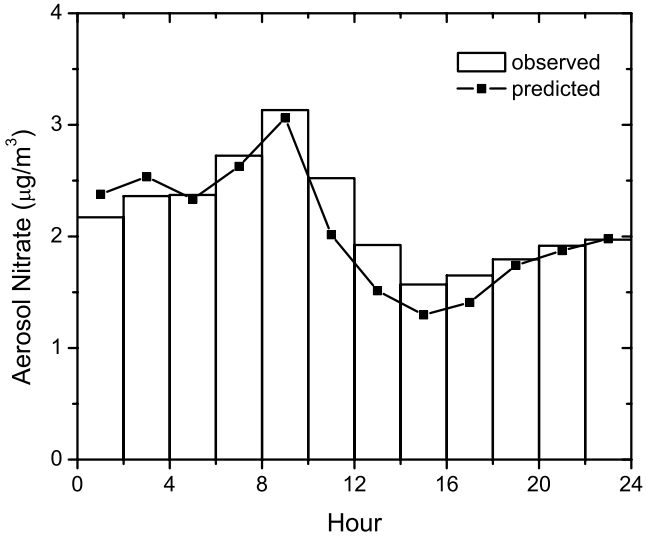

Figure 2. GFEMN prediction versus measurement of aerosol nitrate for January 2002 in Pittsburgh.

[16] Figure 2 shows the comparison between predicted and measured concentrations of aerosol nitrate in the base case simulations; the mean absolute error is 0.2 $\mu g/m^3$ and the model predicts the diurnal variation of aerosol nitrate reasonably well.

3.2. TMR Model Formulation

[17] TMR is an extension of the Eulerian box model described by *Seinfeld and Pandis* [1998]. The concentration of species i in the planetary boundary layer (c_i) is:

$$\frac{dc_i}{dt} = \left(\frac{\partial c_i}{\partial t}\right)_{\text{cond/evap}} - \frac{\nu_i}{H(t)}c_i + \frac{q_i}{H(t)} + R_i + \frac{c_i^0 - c_i}{\tau_r} + \frac{c_i^a - c_i}{H(t)}\frac{dH}{dt}\Phi\left(\frac{dH}{dt}\right), \quad (1)$$

where $(\partial c_i/\partial t)_{\text{cond/evap}}$ is the rate of mass transfer of the species between the gas and particulate phases, ν_i is its dry deposition velocity, H is the mixing height, q_i is its emission rate, R_i is its production rate, c^o is the concentration of the species in the air advected into the box, τ_r is its residence time in the box, and c^a is the concentration of the species above the boundary layer. The unit step function, Φ, allows the incorporation of the entrainment term only when the mixing height is increasing [*Seinfeld and Pandis*, 1998].

[18] Measured concentrations of sulfate and total ammonia are used as inputs by TMR at each time step and the model simulates the evolution of aerosol nitrate and nitric acid. The primary emissions of these species are negligible and therefore $q_i = 0$. For an atmosphere that is relatively homogeneous $c_i \approx c_i^o \approx c_i^a$ and equation 1 is simplified:

$$\frac{dc_i}{dt} = \left(\frac{\partial c_i}{\partial t}\right)_{\text{cond/evap}} - \frac{\nu_i}{H(t)}c_i + R_i. \quad (2)$$

Even if the area of this application is relatively homogeneous [*Tang et al.*, 2004], the term R_i in equation 2 is in general the net generation rate with contributions not only from chemistry but also from horizontal and vertical transport.

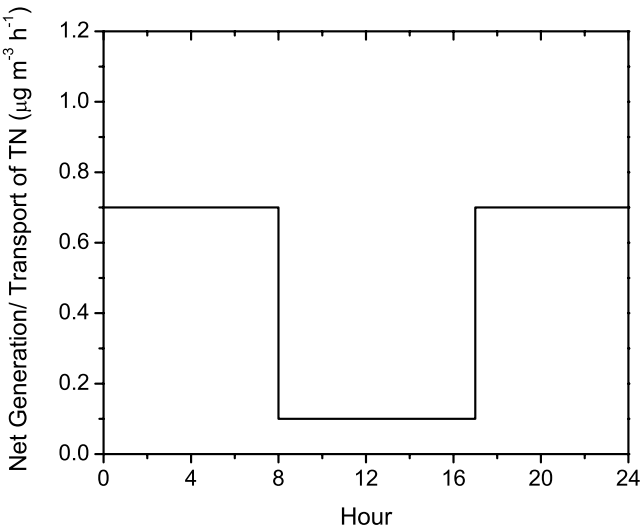

Figure 3. Diurnal profile of nitric acid generation used by TMR for January 2002.

[19] The chemical formation rate can be estimated from other available measurements. Nitric acid is produced primarily by two pathways. In the absence of sunlight, the reaction $NO_2 + O_3 \rightarrow NO_3 + O_2$ is followed by the conversion of NO_3 to N_2O_5 and eventually to HNO_3. Assuming as an upper limit that all of the NO_3 produced by this reaction yields HNO_3, using NO_2 and O_3 measurements from PAQS [*Wittig et al.*, 2004a] and a rate constant recommended by *DeMore et al.* [1997], we estimate a maximum production rate of approximately 1 $\mu g\ m^{-3}\ h^{-1}$ by this pathway. Reactions of the NO_3 radical with NO and organic vapors result in a lower production rate. Using the measured concentrations of NO, NO_2, and O_3 during the nighttime production rates in the range of 0.3–1 $\mu g\ m^{-3}\ h^{-1}$ were estimated. As NO_3 is rapidly photolyzed by UV radiation, during the daytime $NO_2 + OH \rightarrow HNO_3$ becomes the dominant reaction pathway. Measurements of OH concentrations were not available during PAQS; estimates suggest a range of maximum concentrations of 0.5 to 1 $\times\ 10^6$ molecules/cm^3 for the wintertime [*Seinfeld and Pandis*, 1998]. To calculate the rate of HNO_3 production by this mechanism, OH concentrations in this range were linearly scaled to relative UV intensities for the day [*Wittig et al.*, 2004a] and combined with measurements of NO_2 at PAQS [*Wittig et al.*, 2004a] and the reaction rate constant recommended by *Dransfield et al.* [1999]. By this method we estimate daytime average HNO_3 production rates to be in the range of approximately 0.1 to 0.5 $\mu g\ m^{-3}\ h^{-1}$.

[20] Using the measured concentrations of total nitric acid as a guide, we selected as a first approximation a constant nitric acid generation rate of 0.7 $\mu g\ m^{-3}\ h^{-1}$ for the evening hours and early mornings, and a value of 0.2 $\mu g\ m^{-3}\ h^{-1}$ for the daytime (Figure 3). The former value is less than the upper limit of HNO_3 production calculated by the $NO_2 + O_3$ reaction mechanism and is in the expected range. The daytime generation rate is below the range calculated by the NO_2 + OH reaction using assumed OH values; it is likely that in this case, entrainment of cleaner air from the free troposphere may be diluting the air in the planetary boundary when the mixing height is rising during the day.

[21] A dry deposition velocity of 6 cm s^{-1} was calculated for HNO_3 by the method described by *Davidson and Wu* [1990] assuming aerodynamic resistance to be the only barrier to dry deposition, a mean wind velocity at 10 m of 2 m s^{-1} as measured at PAQS, and an effective roughness height of 1 m, which is appropriate for western Pennsylvania. The high deposition velocity of HNO_3 is the result of its high affinity for surfaces (zero surface resistance). Values in the range of 1–8 cm s^{-1} have been reported [*Seinfeld*, 1986]. An average deposition velocity of 0.1 cm s^{-1} for aerosols species was taken from a survey of the literature [*Davidson and Wu*, 1990]. The single value representing the dry deposition velocity of all $PM_{2.5}$ is thought to be the average deposition velocity of a polydisperse aerosol population. The sensitivity of the model to relative deposition rates of gas and aerosol phases will be discussed in a later section. The model assumes a mixing height of 1000 m between 1000 and 1700 EST and 300 m for all other hours in a 24-hour period, inferred from estimates of twice-daily mixing heights [*Holzworth*, 1972] (see also http://weather.uwyo.edu) collected for 0700 and 1900 in Pittsburgh, and hours of sunrise and sunset for the modeling period.

[22] Measurements of sulfate and total ammonium are used as inputs to the model, and equation (2) is solved for $PM_{2.5}$ nitrate and nitric acid. Instead of solving the condensation/evaporation equation to calculate partitioning between gas and aerosol phases, the system is assumed to be in equilibrium. *Takahama et al.* [2004] argue that this equilibrium assumption is reasonable for $PM_{2.5}$ in western Pennsylvania. Because of the difference in timescales involved in the processes equation (1), the model is solved by the operator splitting method [*Oran and Boris*, 2001] where the equilibrium module GFEMN solves the phase partitioning part and the generation and removal processes are solved by the Euler method. To check for problems of convergence and stability, the integration algorithm was tested using increasingly smaller values for the time step until the solutions to the equations no longer changed within a reasonable margin of error. An operator time step of one hour was determined to be sufficiently accurate for this study.

[23] To determine solutions to equation (2) for different emission scenarios that do not depend on the initial conditions of the simulation, the meteorological inputs, sulfate, total ammonia, and total nitric acid generation were assumed to be periodic, with each function assuming values over its 24-hour period as described above. Under such conditions, TMR reaches a dynamic quasi-stationary state in a relatively small number of iterations, in which the diurnal cycle does not change from one simulation day to the next. Figure 4 shows the total nitric acid profile approaching this steady state cycle after 24 hours for the base case scenario. Concentrations from this steady state cycle are used to calculate average $PM_{2.5}$ and species concentrations.

[24] In the TMR simulations presented, we assumed that the changes in the gas/aerosol phase partitioning of ammonia do not affect significantly its total (gas and aerosol) concentrations. This becomes necessary because of the complex interactions of ammonia with the ground. The

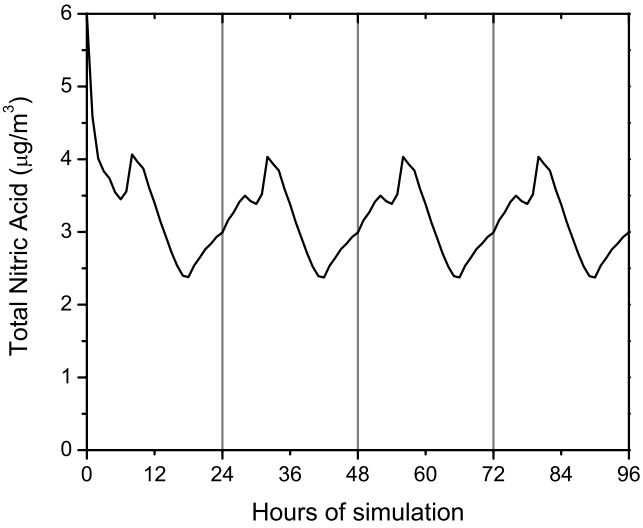

Figure 4. TMR converging on dynamic quasi-stationary state.

surface exchange of ammonia is governed in part by a compensation point [*Farquhar et al.*, 1980], or a local surface concentration below which the direction of ammonia flux changes from deposition to emission, with the ammonia deposition velocity becoming increasingly small as the gas-phase concentrations approach the compensation point [*Asman*, 1998]. The compensation point reported in the literature varies from 0 to 4 $\mu g/m^3$, and depends on the surface vegetation or surface type as well as meteorological conditions, with winter conditions generally favoring lower compensation points. The mean gas-phase concentrations are less than 0.4 $\mu g/m^3$ for our range of simulations, in the same general range as the expected compensation points.

[25] Figures 5a and 5b show the predicted total nitric acid and aerosol nitrate concentrations by TMR for the base case simulation. The mean absolute error for total nitric acid is 0.3 $\mu g/m^3$. The observed aerosol nitrate is reproduced with a mean error of 0.1 $\mu g/m^3$.

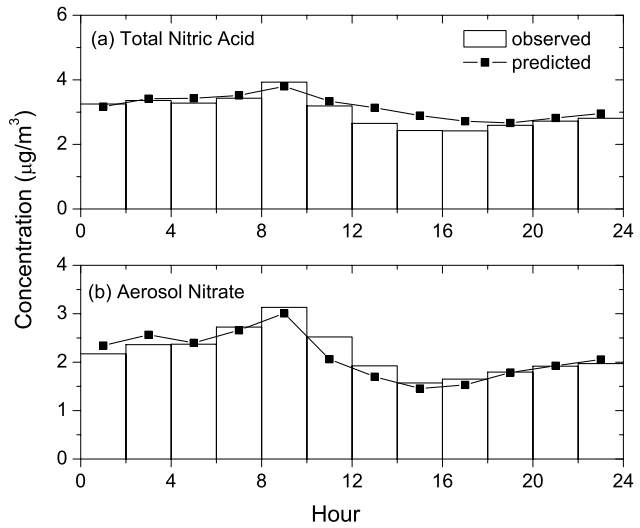

Figure 5. TMR prediction versus measurements of (a) total nitric acid and (b) aerosol nitrate for January 2002 in Pittsburgh.

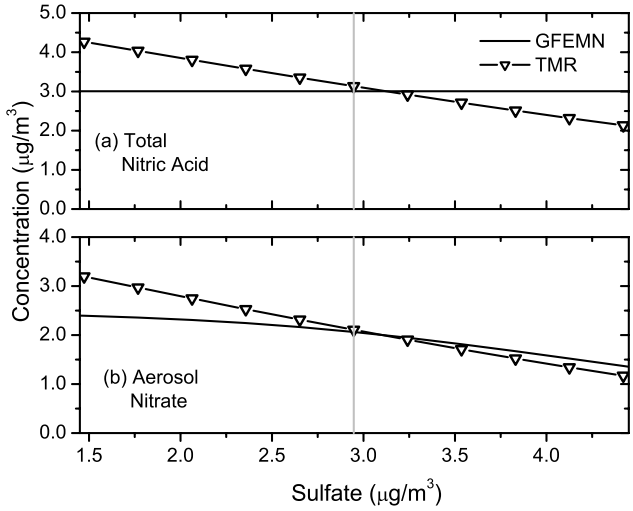

Figure 6. Response of (a) total nitric acid and (b) aerosol nitrate to changes in sulfate concentrations by TMR and GFEMN. Vertical lines indicate conditions for the base case scenario.

4. Results

[26] In the following simulations, concentrations of sulfate and total ammonia and also the total nitric acid generation rate are varied from −50 to 50% of the original value.

4.1. Response to Changes in Sulfate Concentrations

[27] The effect of changes in sulfate concentrations on total nitric acid is shown in Figure 6a. GFEMN assumes that a change in one component has no effect on the others and therefore the average total nitric acid (over the 24-hour steady state cycle) remains constant at 3 $\mu g/m^3$. Meanwhile, TMR predicts that the total nitric acid concentration increases by 0.77 $\mu g/m^3$ for every $\mu g/m^3$ of sulfate reduced in the system because of the feedback of gas/aerosol partitioning on the total nitric acid availability. Because of the low temperatures observed in Pittsburgh during the winter, when sulfate is reduced and the quantity of ammonia available to react with nitric acid increases, more ammonium nitrate is formed. Figure 6b shows that when sulfate concentrations are reduced by 20%, GFEMN predicts that the concentration of aerosol nitrate increases from 2.1 $\mu g/m^3$ from the base case up to 2.3 $\mu g/m^3$. For the same 20% sulfate reduction, TMR predicts that the aerosol nitrate concentration increases from 2.1 $\mu g/m^3$ in the base case up to 2.5 $\mu g/m^3$. For a 50% reduction in sulfate, TMR predicts that the aerosol nitrate concentration will be 3.2 $\mu g/m^3$, which is 35% more than the 2.4 $\mu g/m^3$ that GFEMN predicts.

[28] When sulfate is reduced, TMR generally predicts that more aerosol nitrate will be formed than GFEMN predicts. The increasing fraction of total nitric acid partitioned into the aerosol phase results in higher total nitric acid concentrations; higher partial pressures of nitric acid result in higher aerosol nitrate concentrations. When sulfate is increased, on the other hand, TMR predicts less of both total

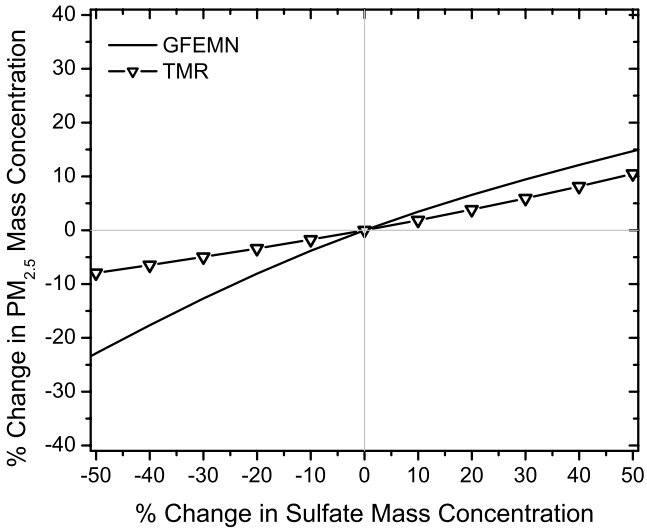

Figure 7. Response of inorganic $PM_{2.5}$ (plotted as the sum of components without water) to changes in sulfate concentrations.

nitric acid and aerosol nitrate than GFEMN. In this case more ammonia becomes associated with the sulfate and more nitric acid exists in the gas phase. As Figure 6a shows, while total nitric acid concentrations remain constant according to GFEMN, total nitric acid decreases by 0.68 $\mu g/m^3$ for every $\mu g/m^3$ of sulfate added to the system. The difference between GFEMN and TMR predictions of aerosol nitrate concentrations are not as dramatic for the case of sulfate reductions, as Figure 6b shows. The results are somewhat similar because in this concentration regime, the change in sulfate concentrations imposed on both models affects the aerosol nitrate concentration more than the change in total nitric acid. Thus, for a 20% increase in sulfate, the difference between aerosol nitrate predicted by the two models is 6%, and for a 50% increase in sulfate the difference is 15%.

[29] The effect of changing sulfate concentrations on inorganic $PM_{2.5}$ mass concentrations can be seen in Figure 7. In the ideal case where there is no substitution of nitrate for sulfate in aerosols, $PM_{2.5}$ would be reduced by 1.34 $\mu g/m^3$ as ammonium sulfate for every $\mu g/m^3$ of sulfate removed from the system. The PM response is defined as the change in $PM_{2.5}$ concentration with respect to the change in sulfate concentration, i.e., $\Delta PM/\Delta TS$. *Ansari and Pandis* [1998] defined a PM response between 1.0 and 1.34 $\mu gPM_{2.5}/\mu gTS$ as being "linear" and PM responses between 0 and 1.0 $\mu gPM_{2.5}/\mu gTS$ as "nonlinear." We will adapt this convention here. The PM responses predicted by GFEMN for 20% and 50% reductions in sulfate are 0.84 and 1.16 $\mu gPM_{2.5}/\mu gTS$, respectively, indicating that there is a transition from a nonlinear to linear response. This transition occurs because for larger reductions of sulfate there is little nitric acid left to be pulled into the aerosol phase; reductions in $PM_{2.5}$ then occur mainly as reductions in ammonium sulfate. According to TMR, however, the PM response remains nonlinear (below 0.40 $\mu gPM_{2.5}/\mu gTS$) for the entire range of sulfate reductions (down to 50%) in our simulations. This is again because of the fact that TMR predicts more nitrate to replace sulfate in the aerosol because of the increased availability of total nitric acid. For reductions in sulfate concentrations of 50%, GFEMN and TMR predict reductions in $PM_{2.5}$ of 23% and 8%, respectively. As sulfate concentrations are increased, ammonium sulfate and ammonium bisulfate compete for the available ammonium and drive nitrate into the gas phase. Thus reductions in aerosol nitrate have the effect of offsetting increases in sulfate, and both models predict the PM response to be less than one. For a 50% increase in sulfate, the $PM_{2.5}$ mass concentration is predicted to increase by modest amounts of 15 and 10% by GFEMN and TMR, respectively.

4.2. Response to Changes in Total Ammonia Concentrations

[30] The response of total nitric acid to changes in total ammonia concentrations is shown in Figure 8a. GFEMN assumes a constant total nitric acid concentration of 3.0 $\mu g/m^3$, while TMR predicts that on average, the total nitric acid will be reduced by 2.3 $\mu g/m^3$ for every $\mu g/m^3$ of total ammonia reduced. For 20 and 50% reductions in ammonia, GFEMN predicts the aerosol nitrate concentrations to be 1.42 and 0.34 $\mu g/m^3$ (Figure 8b), respectively. For corresponding reductions in ammonia, TMR predicts aerosol nitrate concentrations 0.21 $\mu g/m^3$ and 0.12 $\mu g/m^3$ lower than GFEMN. The difference in predictions between the two models is small because when total ammonia is reduced, ammonium nitrate formation becomes limited by ammonia and therefore is more sensitive to changes in total ammonia than total nitric acid. Though by a small amount, TMR consistently predicts concentrations below that of GFEMN because of the feedback of decreasing aerosol nitrate concentrations on the total nitric acid concentrations. When total ammonia concentrations are increased, GFEMN still assumes a constant total nitric acid concentration, while TMR predicts that it will increase by 3.2 $\mu g/m^3$ for every $\mu g/m^3$ of total ammonia added to the system. For 20 and 50% increases in total ammonia, GFEMN predicts aerosol nitrate concentrations of 2.45

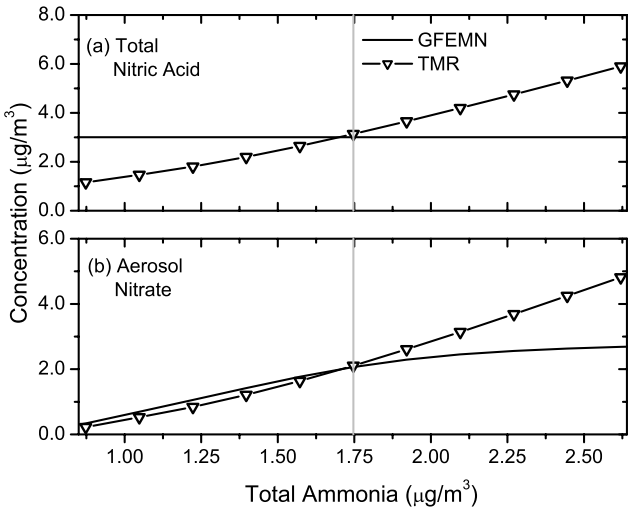

Figure 8. Response of (a) total nitric acid and (b) aerosol nitrate to changes in ammonia concentrations by TMR and GFEMN. Vertical lines indicate conditions for the base case scenario.

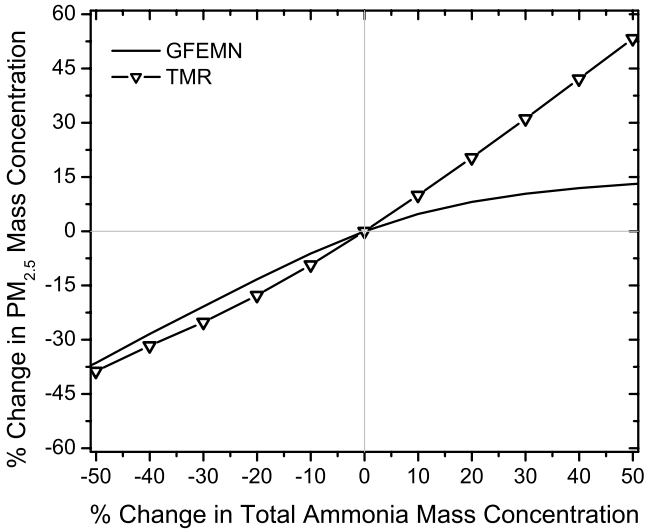

Figure 9. Response of inorganic $PM_{2.5}$ (plotted as the sum of components without water) to changes in ammonia concentrations.

and 2.68 $\mu g/m^3$, respectively; TMR predicts nitrate concentrations 0.69 and 2.14 $\mu g/m^3$ higher than GFEMN for these cases. At total ammonia concentrations 50% higher than the base case, 90% of the total nitric acid is in the aerosol phase in the GFEMN system, while only 83% of it is in the aerosol phase according to TMR, suggesting that as ammonia concentrations are increased, ammonium nitrate formation is limited by the total nitric acid concentration in simulations with GFEMN more so than with TMR.

[31] Figure 9 shows how $PM_{2.5}$ concentrations respond to changes in total ammonia concentrations relative to the base case. For reductions in total ammonia of 20 and 50%, the $PM_{2.5}$ is reduced by 13 and 36% according to GFEMN and 18 and 39% according to TMR, respectively. This reduction is mainly achieved through the reduction of ammonium nitrate. When total ammonia is increased by 20 and 50%, the $PM_{2.5}$ concentration is predicted to increase by only 8 and 13% by GFEMN but by 20 and 53% by TMR, respectively. For each model, increasing total ammonia is qualitatively similar to decreasing sulfate concentrations, as both scenarios lead to an increase of the total ammonia to sulfate ratio, which is a metric often used to describe the composition domain for classification into regions of similar thermodynamic responses [*Ansari and Pandis*, 1999; *Zhang et al.*, 2000]. As Figures 6b and 8b show, when total ammonia concentrations relative to sulfate increase, the concentration of aerosol nitrate is also increased. For a given set of meteorological conditions and the same total ammonia to sulfate ratio, however, quantitative predictions from each model depend on the difference between the total ammonia and sulfate rather than their ratios, so the actual response of aerosol nitrate and $PM_{2.5}$ depends on which variable, total ammonia or sulfate, is varied.

4.3. Response to Changes in Total Nitric Acid Generation Rate

[32] TMR can also be used to make first-order approximation of how changes in total HNO_3 concentrations can impact $PM_{2.5}$ concentrations by making adjustments in the net generation rate, R, in equation (2).

[33] For the same total nitric acid concentrations (and all other variables remaining the same), GFEMN and TMR are identical in every respect except that gas/aerosol partitioning affects the total nitric acid concentration in the TMR system; for a given concentration of total nitric acid, the two models will predict the same $PM_{2.5}$ concentration. When R is varied from −50 to 50%, total nitric acid concentrations are almost linear in R (correlation coefficient = 0.999) for the range of our changes. Plotted in Figure 10 is the change in $PM_{2.5}$ mass concentration as a function of the change in R and in total nitric acid. Only one curve is shown because for the same variations in total nitric acid concentrations, GFEMN will trace the same response curve as TMR. For 20 and 50% reductions in R, which correspond to 22 and 60% reductions in total nitric acid, the $PM_{2.5}$ mass concentration is reduced by 7 and 21% from the base case, respectively. The PM response curve is concave because there is more nitric acid than free ammonia initially, and the full extent of total nitric acid reduction is not realized until enough nitric acid is removed such that it becomes the limiting reactant in the formation of ammonium nitrate. For 20 and 50% increases in R, which correspond to 21 and 54% increases in total nitric acid, the $PM_{2.5}$ increases by 5 and 9%, respectively. As more nitric acid is introduced into the system, more ammonium nitrate is predicted to form, but this quantity eventually becomes limited by ammonia availability.

4.4. Changes to Phase State After Emission Changes

[34] In all of the simulations, the particles were assumed to be liquid because the relative humidities of the average day in January remained above the observed crystallization RH. If the particles were assumed to follow the deliquescence curve, the predictions for TMR would change

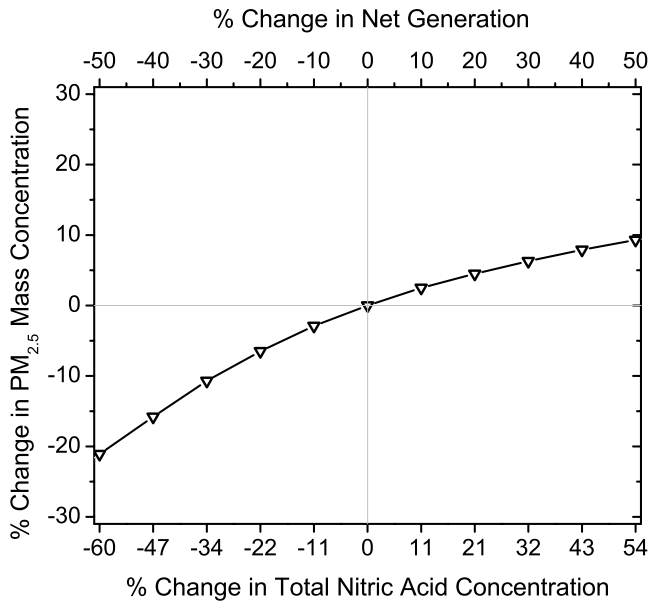

Figure 10. Response of inorganic $PM_{2.5}$ to changes in total nitric acid generation rate and corresponding total nitric acid concentrations.

dramatically, though not so much for GFEMN. For instance, in TMR base case simulations, deliquescence predictions of $PM_{2.5}$ are lower than efflorescence predictions by 29%, and deliquescence predictions of $PM_{2.5}$ can be as much as 51% lower in the range of our simulations when the total ammonia to sulfate ratio is increased. With GFEMN the difference is 7% in the base case and the maximum only 15% with deliquescence branch simulations consistently predicting lower than efflorescence branch. These differences occur because the mutual deliquescence RH of ammonium sulfate and ammonium nitrate at these temperatures is around 70%, and therefore the phase state predicted is different if deliquescence is assumed. Because the ammonium nitrate dissociation constant is higher for a solid particle than a liquid particle at moderate to high RHs, less ammonium nitrate aerosol is predicted to form in the solid case. In the TMR simulations, this phenomenon is exacerbated by the fact that more nitric acid rapidly deposits when less aerosol is formed; consequently there is less nitric acid available to saturate the gas phase with ammonia to form ammonium nitrate. Since the total nitric acid is constant in the GFEMN simulations, this feedback of nitric acid removal on phase equilibrium is neglected, and therefore the difference is limited to the difference in the dissociation constant between liquid and solid aerosol only and not the quantity of nitric acid in the system.

[35] Measurements of aerosol water content indicate that particles were liquid below the mutual deliquescence point of sulfate and nitrate for January 2002, suggesting that particles were metastable during the winter, and crystallization and not deliquescence governed the phase state of the particles. Furthermore, for the base case simulations, both GFEMN and TMR are able to reproduce the observed concentrations of aerosol nitrate from the partitioning of total nitric acid better when the aerosols are assumed to lie on the efflorescence branch. The prevalence of metastable aerosols in general is also reported by *Rood et al.* [1989]. *Zhang et al.* [2003] found that in their evaluation of inorganic measurements during the Atlanta Supersite Experiment, assuming deliquescence returned "unrealistic" partitioning of nitrate and nitric acid.

[36] The change in phase state of the particles when the chemical composition of the system changes is a potentially important issue. The crystallization RH is a function of temperature and chemical composition of the aerosol. *Martin et al.* [2003] found that for a NH_4^+-NO_3^--SO_4^{2-}-H^+ system at 293 K, the crystallization RH is lowered when (1) the sulfate fraction of anions is reduced, and when (2) the ammonium fraction of cations is reduced. These findings agree with our current knowledge of the hygroscopic properties of single-component particles. For a fixed level of ammonium in the aerosol, as the sulfate fraction of anions is reduced, the chemical character of the aerosol moves away from ammonium sulfate and approaches that of ammonium nitrate. Since the CRH of ammonium nitrate is extremely low reducing the sulfate fraction of anions lowers the CRH. Furthermore, for a fixed quantity of sulfate, when the ammonium fraction of cations is reduced, the aerosol becomes more acidic, since acidic aerosols are generally more hygroscopic than nonacidic aerosols, so the CRH should decrease. If such trends hold at lower temperatures observed during the winter, the simulated aerosols would remain above the CRH and thus unchanged in physical state when sulfate is reduced; a similar result would be expected for the case of reductions in ammonia. The effect of reducing nitrate is not as clear, as both the sulfate fraction and ammonium fraction would be changed. However, mineral dusts within aqueous particles can increase crystallization RHs by providing sites for heterogeneous nucleation [*Martin et al.*, 2001; *Han et al.*, 2002], and the role of organics in crystallization is uncertain. Therefore we have imposed the assumption that the phase state of the particles remain the same as in the base case during our simulations, but given the sensitivity of our predictions to the assumed phase state, it is apparent that gaining a better understanding of phase transitions of aerosols as they occur in the atmosphere is important.

4.5. Sensitivity to Relative Deposition Velocities

[37] The TMR results are fairly robust with respect to the aerosol and nitric acid deposition velocities chosen. The ratio of the nitric acid deposition velocity to that of the aerosol used in the original TMR simulations is 60. Between the ratios of 30 to 120, $PM_{2.5}$ predictions by TMR differ by no more than 1%, with the largest differences occurring at high total ammonia to sulfate ratios. As this ratio of deposition velocities approaches unity, the TMR predictions approach those of GFEMN, which is the expected outcome as the implicit assumption in the GFEMN simulations is that the deposition velocities of the aerosol and gas phases are the same. These findings are consistent with those of *Pandis and Seinfeld* [1990] and *Seinfeld and Pandis* [1998] who found that when the ratio of the gas-phase deposition velocity to that of the aerosol is increased from 10 to 100, only "minor effects" are observed in their metric of cumulative deposition.

5. Conclusions

[38] An observation-based Eulerian box model, TMR, was introduced to evaluate the response of $PM_{2.5}$ mass concentrations to changes in concentrations of sulfate, total ammonia, and total nitric acid. By using measurements as inputs, TMR avoids the use of uncertain emission inventories. TMR assumes that particles are in equilibrium with the gas phase, but the removal rate of total nitric acid from the system is dependent on its partitioning between the gas and aerosol phases.

[39] Using measurements collected in the Pittsburgh Air Quality Study, an "average" day for January 2002 was constructed and used as the base case scenario for simulations. Predictions of $PM_{2.5}$ response to changes in precursor concentrations (relative to the base case) were compared with predictions from a chemical equilibrium model, GFEMN, as used in the approach of *Ansari and Pandis* [1998]. Use of thermodynamic models like GFEMN for simulation of future scenarios implicitly assumes that partitioning has no effect on the total nitric acid concentration.

[40] For scenarios that lead to higher total ammonia to sulfate ratios, i.e., reductions in sulfate and increases in total ammonia, TMR predicts more aerosol nitrate to form than GFEMN because the transformation of gas-phase nitric acid and ammonia to ammonium nitrate increases the lifetime and concentration of total nitric acid in the system. For a

50% decrease in sulfate, GFEMN predicts that the $PM_{2.5}$ concentration will be reduced by 23%, while TMR predicts that the reduction will be 8%. The results from TMR suggest that when partitioning affects the lifetime of total nitric acid, significant increases in ammonium nitrate may partially offset benefits of sulfate reductions alone in low-temperature conditions as seen in the wintertime in Pittsburgh.

[41] When the total ammonia concentration is increased by 50%, GFEMN predicts a 13% increase in $PM_{2.5}$ while TMR predicts a 53% increase, suggesting that the system as modeled by TMR is more sensitive to levels of total ammonia.

[42] For increases in sulfate and reductions in total ammonia, which lead to ammonia-poor conditions, TMR predicts lower total nitric acid concentrations than GFEMN, but the predictions of aerosol nitrate and $PM_{2.5}$ concentrations between the two models are similar.

[43] On average, the total nitric acid concentration varies almost linearly with the magnitude of the net generation rate. When the net generation for nitric acid is changed, the $PM_{2.5}$ concentration responds accordingly. For a 50% reduction in the net generation, which corresponds to a reduction in total nitric acid concentration of 60%, the $PM_{2.5}$ decreases by 21%. For the same level of total nitric acid concentrations, GFEMN and TMR predictions are the same because the two models are identical in every respect except the inclusion of feedback of partitioning on total nitric acid concentrations in TMR.

[44] Model predictions of GFEMN and especially TMR are sensitive to the assumed physical state of the aerosol. If particles were allowed to become solid below the mutual DRH during our simulations, the difference in aerosol nitrate predictions could be as great as 15% for GFEMN and 51% for TMR in the range of our simulations. How the crystallization RH will actually change with the composition of the aerosol is very uncertain. *Martin et al.* [2003] characterized the crystallization RHs for particles composed of ammonium, nitrate, and sulfate at room temperature (293 K), but the role of organics and other species neglected in partitioning calculations is unclear, and especially at the low temperatures observed during the wintertime in Pittsburgh.

[45] The TMR model predictions are robust with respect to assumed deposition velocities, however. For the base case simulations, the ratio of gas-phase to aerosol-phase deposition velocities used was 60; when this value varies from 30 to 120 the influence on the outcome is no more than 1%.

[46] **Acknowledgments.** This research was conducted as part of the Pittsburgh Air Quality Study, which was supported by U.S. Environmental Protection Agency under contract R82806101 and the U.S. Department of Energy National Energy Technology Laboratory under contract DE-FC26-01NT41017. This paper has not been subject to EPA's peer and policy review and therefore does not necessarily reflect the views of the agency. No official endorsement should be inferred. This work benefited from the comments of Peter J. Adams, Neil M. Donahue, and Andrey Y. Khlystov.

References

Ansari, A. S., and S. N. Pandis (1998), Response of inorganic $PM_{2.5}$ to precursor concentrations, *Environ. Sci. Technol.*, *32*, 2706–2714.

Ansari, A. S., and S. N. Pandis (1999), Prediction of multicomponent inorganic atmospheric aerosol behavior, *Atmos. Environ.*, *33*, 745–757.

Asman, W. A. H. (1998), Factors influencing local dry deposition of gases with special reference to ammonia, *Atmos. Environ.*, *32*, 415–421.

Bassett, M., and J. H. Seinfeld (1983), Atmospheric equilibrium model of sulfate and nitrate aerosols, *Atmos. Environ.*, *17*, 2237–2252.

Blanchard, C. L., and G. M. Hidy (2003), Effects of changes in sulfate, ammonia, and nitric acid on particulate nitrate concentrations in the southeastern United States, *J. Air Waste Manage. Assoc.*, *53*, 283–290.

Davidson, C. I., and Y. L. Wu (1990), Dry deposition of particles and vapors, in *Acid Precipitation*, vol. 3, edited by S. E. Lindberg, A. L. Page, and S. A. Norton, pp. 103–216, Springer, New York.

DeMore, W. B., S. P. Sanders, D. M. Golden, R. F. Hampson, M. J. Kurylo, C. J. Howard, A. R. Ravishankara, C. E. Kolb, and M. J. Molina (1997), Chemical kinetics and photochemical data for use in stratospheric modeling: Evaluation 14, *JPL Publ. 02-25*.

Dransfield, T. J., K. K. Perkins, N. M. Donahue, J. G. Anderson, M. M. Sprengnether, and K. L. Demerjian (1999), Temperature and pressure dependent kinetics of the gas-phase reaction of the hydroxyl radical with nitrogen dioxide, *Geophys. Res. Lett.*, *26*, 687–690.

Farquhar, G. D., P. M. Firth, R. Wetselaar, and B. Weir (1980), On the gaseous exchange of ammonia between leaves and the environment—Determination for the ammonia compensation point, *Plant Physiol.*, *66*, 710–714.

Han, J., H. Hung, and S. T. Martin (2002), Size effect of hematite and corundum inclusions on the efflorescence relative humidities of aqueous ammonium nitrate particles, *J. Geophys. Res.*, *107*(D10), 4086, doi:10.1029/2001JD001054.

Holzworth, G. C. (1972), Mixing heights, wind speeds, and potential for urban air pollution throughout the contiguous United States, *Publ. AP-101*, Off. of Air Programs, U.S. Environ. Protect. Ag., Research Triangle Park, N. C.

Intergovernmental Panel on Climate Change (IPCC) (2001), *Climate Change 2001: The Scientific Basis, Contribution of Working Group I to the Third Assessment Report of the Intergovernmental Panel on Climate Change*, edited by J. T. Houghton et al., 881 pp., Cambridge Univ. Press, New York.

Jacobson, M. Z., A. Tabazadeh, and R. P. Turco (1996), Simulating equilibrium within aerosols and nonequilibrium between gases and aerosols, *J. Geophys. Res.*, *101*, 9079–9091.

Khlystov, A., C. O. Stanier, S. Takahama, and S. N. Pandis (2005), Water content of ambient aerosol during the Pittsburgh Air Quality Study, *J. Geophys. Res.*, *110*, D07S10, doi:10.1029/2004JD004651.

Kim, Y. P., J. H. Seinfeld, and P. Saxena (1993), Atmospheric gas-aerosol equilibrium I. Thermodynamic model, *Aerosol Sci. Technol.*, *19*, 157–181.

Martin, S. T., J. H. Han, and H. M. Hung (2001), The size effect of hematite and corundum inclusions on the efflorescence relative humidities of aqueous ammonium sulfate particles, *Geophys. Res. Lett.*, *28*, 2601–2604.

Martin, S. T., J. C. Schlenker, A. Malinowski, H. Hung, and Y. Rudich (2003), Crystallization of atmospheric sulfate-nitrate-ammonium particles, *Geophys. Res. Lett.*, *30*(21), 2102, doi:10.1029/2003GL017930.

Meng, Z., J. H. Seinfeld, P. Saxena, and Y. P. Kim (1995), Atmospheric gas-aerosol equilibrium: IV, Thermodynamics of carbonates, *Aerosol Sci. Technol.*, *23*, 131–154.

Nenes, A., C. Pilinis, and S. N. Pandis (1999), Continued development and testing of a new thermodynamic aerosol module for urban and regional air quality models, *Atmos. Environ.*, *33*, 1553–1560.

North American Research Strategy for Tropospheric Ozone (NARSTO) (2003), Particulate matter science for policy makers—A NARSTO assessment. Part 2, NARSTO Manage. Off., Pasco, Wash. (Available at http://www.cgenv.com/NARSTO.).

Oran, E. S., and J. P. Boris (2001), *Numerical Simulation of Reactive Flow*, 2nd ed., Cambridge Univ. Press, New York.

Pandis, S. N., and J. H. Seinfeld (1990), On the interaction between equilibration processes and wet or dry deposition, *Atmos. Environ.*, *24*, 2313–2327.

Pilinis, C., and J. H. Seinfeld (1987), Continued development of a general equilibrium model for inorganic multicomponent atmospheric aerosols, *Atmos. Environ.*, *22*, 1985–2001.

Pun, B. K., and C. Seigneur (2001), Sensitivity of particulate matter nitrate formation to precursor emissions in the California San Joaquin Valley, *Environ. Sci. Technol.*, *35*, 2979–2987.

Rees, S. L., A. L. Robinson, A. Khlystov, C. O. Stanier, and S. N. Pandis (2004), Mass balance closure and the federal reference method for $PM_{2.5}$ in Pittsburgh, Pennsylvania, *Atmos. Environ.*, *38*, 3305–3318.

Rood, M. J., M. A. Shaw, T. V. Larson, and D. S. Covert (1989), Ubiquitous nature of ambient metastable aerosol, *Nature*, *337*, 537–539.

Russell, A. G., and G. R. Cass (1986), Verification of a mathematical model for aerosol nitrate and nitric acid formation and its use for control measure evaluation, *Atmos. Environ.*, *20*, 2011–2025.

Saxena, P., A. B. Hudischewskyj, C. Seigneur, and J. H. Seinfeld (1986), A comparative study of equilibrium approaches to the chemical characterization of secondary aerosols, *Atmos. Environ.*, *20*, 1471–1483.

Seigneur, C. (2001), Current status of air quality models for particulate matter, *J. Air Waste Manage. Assoc.*, *51*, 1508–1521.

Seinfeld, J. H. (1986), *Atmospheric Chemistry and Physics of Air Pollution*, John Wiley, Hoboken, N. J.

Seinfeld, J. H., and S. N. Pandis (1998), *Atmospheric Chemistry and Physics*, John Wiley, Hoboken, N. J.

Takahama, S., A. E. Wittig, D. V. Vayenas, C. I. Davidson, and S. N. Pandis (2004), Modeling the diurnal variation of nitrate during the Pittsburgh Air Quality Study, *J. Geophys. Res.*, *109*, D16S06, doi:10.1029/2003JD004149.

Tang, W., T. Raymond, A. E. Wittig, C. I. Davidson, S. N. Pandis, A. L. Robinson, and K. Crist (2004), Spatial variations of $PM_{2.5}$ during the Pittsburgh Air Quality Study, *Aerosol Sci. Technol.*, *38*, suppl. 2, 80–90.

U.S. Environmental Protection Agency (1996), Air Quality Criteria for Particulate Matter, *Rep. EPA/600/P-95/001aF*, vol. 1, U.S. Govt. Print. Off., Washington, D. C.

West, J. J., A. S. Ansari, and S. N. Pandis (1999), Marginal PM2.5: Nonlinear aerosol mass response to sulfate reductions in the eastern United States, *J. Air Waste Manage. Assoc.*, *49*, 1415–1424.

Wexler, A. S., and S. L. Clegg (2002), Atmospheric aerosol models for systems including the ions H^+, NH_4^+, Na^+, SO_4^{2-}, NO_3^-, Cl^-, Br^-, and H_2O, *J. Geophys. Res.*, *107*(D14), 4207, doi:10.1029/2001JD000451.

Wittig, A. E., N. Anderson, A. Khlystov, S. N. Pandis, C. Davidson, and A. L. Robinson (2004a), Pittsburgh Air Quality Study overview, *Atmos. Environ.*, *38*, 3107–3125.

Wittig, A. E., S. Takahama, A. Y. Khlystov, S. N. Pandis, S. Hering, B. Kirby, and C. I. Davidson (2004b), Semi-continuous $PM_{2.5}$ inorganic composition measurements during the Pittsburgh Air Quality Study, *Atmos. Environ.*, *38*, 3201–3213.

Zhang, J., W. L. Chameides, R. Weber, G. Cass, D. Orsini, E. Edgerton, P. Jongejan, and J. Slanina (2003), An evaluation of the thermodynamic equilibrium assumption for fine particulate composition: Nitrate and ammonium during the 1999 Atlanta Supersite Experiment, *J. Geophys. Res.*, *108*(D7), 8414, doi:10.1029/2001JD001592.

Zhang, Y., C. Seigneur, J. H. Seinfeld, M. Jacobson, S. L. Clegg, and F. S. Binkowski (2000), A comparative review of inorganic aerosol thermodynamic equilibrium modules: Similarities, differences, and their likely causes, *Atmos. Environ.*, *34*, 117–137.

C. I. Davidson, Department of Civil and Environmental Engineering, Carnegie Mellon University, 5000 Forbes Avenue, Pittsburgh, PA 15213, USA.

S. N. Pandis and S. Takahama, Department of Chemical Engineering, Carnegie Mellon University, 5000 Forbes Avenue, Pittsburgh, PA 15213, USA. (spyros@andrew.cmu.edu)

D. Vayenas, Department of Environmental and Natural Resources Management, University of Ioannina, 2 Seferi Street, GR-30100 Agrinio, Greece.